Atom Optics Realization of the Quantum δ-Kicked Rotor

F. L. Moore,* J. C. Robinson, C. F. Bharucha, Bala Sundaram, and M. G. Raizen
Department of Physics, The University of Texas at Austin, Austin, Texas 78712-1081
(Received 21 July 1995)

We report the first direct experimental realization of the quantum δ-kicked rotor. Our system consists of a dilute sample of ultracold sodium atoms in a periodic standing wave of near-resonant light that is pulsed on periodically in time to approximate a series of delta functions. Momentum spread of the atoms increases diffusively with every pulse until the "quantum break time" after which exponentially localized distributions are observed. Quantum resonances are found for specific values of the pulse period.

PACS numbers: 05.45.+b, 32.80.Pj, 42.50.Vk, 72.15.Rn

The classical kicked rotor or the equivalent standard mapping is a textbook paradigm for Hamiltonian chaos [1]. The quantum δ-kicked rotor (QKR) has played an equally important role for the field of quantum chaos, and a wide range of effects have been predicted [2]. In this Letter we report the first direct experimental realization of the QKR, and the first observation of the onset of dynamical localization in time, the quantum break time, and quantum resonances. Our system consists of a sample of ultracold sodium atoms exposed to a one-dimensional spatially periodic potential that is pulsed on periodically in time. The control of experimental parameters enables a quantitative comparison to theory and opens up many possibilities for future studies.

To describe our system we begin with a two level atom (transition frequency ω_0) interacting with a standing wave of near-resonant light (frequency ω_L). For sufficiently large detuning $\delta_L = \omega_0 - \omega_L$ (relative to the natural linewidth), the excited state amplitude can be adiabatically eliminated. This leads to a conservative Hamiltonian for the ground state $H = p^2/2M - (\hbar\Omega_{\text{eff}}/8)\cos 2k_L x$, where the effective Rabi frequency is $\Omega_{\text{eff}} = \Omega^2/\delta_L$ and k_L is the wave number. ($\Omega/2$ is the resonant Rabi frequency, proportional to the square root of the standing wave intensity.) We now assume that the potential term in the Hamiltonian is multiplied by $f(t)$, a train of N pulses with unit peak heights and period T. The nonzero pulse widths lead to a finite number of resonances in the classical dynamics [3], which limits the diffusion resulting from overlapping resonances to a band in momentum. However, by decreasing the pulse duration with constant area, the width of this band can be made arbitrarily large, approaching the δ-function pulse limit. We illustrate this by considering a train of Gaussian pulses. The Hamiltonian is given by

$$H = \rho^2/2 - k\cos\phi \sum_{n=0}^{N} e^{-(t-n)^2/2\alpha^2}, \qquad (1)$$

where the scaled units $\phi = 2k_L x$, $\rho = (2k_L T/M)p$, $t' = t/T$, and $H' = \left(4k_L^2 T^2/M\right)H$ (primes have been dropped); T is the spacing between the pulses; α is the pulse width; and $k = \Omega_{\text{eff}}\omega_r T^2$ where $\omega_r = \hbar k_L^2/2M$ is the recoil frequency. In the quantized model ϕ and ρ are the conjugate variables satisfying the commutation condition $[\phi, \rho] = i\bar{k}$, where $\bar{k} = 8\omega_r T$.

In these units, the time dependent potential (for an infinite train of pulses) can be rewritten as a discrete Fourier series, leading to

$$H = \frac{\rho^2}{2} - \sqrt{2\pi}\alpha k \sum_{r=-\infty}^{\infty} e^{-2\pi^2\alpha^2 r^2}\cos(\phi - 2\pi r t). \qquad (2)$$

The resonances are located at $\rho = d\phi/dt = 2\pi r$ and the widths of successive resonances fall off because of the exponential factor, thus defining the borders to diffusion as Kolmogorov-Arnold-Moser curves (quasi-integrable behavior). The falloff is governed by the pulse width, parametrized by α. In the limiting case of zero width such that the area under the pulse remains fixed, i.e., $\alpha \to 0, k \to \infty$ such that αk remains finite, all the Fourier weights are equal and using the Poisson sum rule, one gets $H = \rho^2/2 - \kappa\cos\phi\sum_{n=-\infty}^{\infty}\delta(t-n)$, which is the kicked rotor with classical stochasticity parameter $\kappa = \sqrt{2\pi}\alpha k$. Note that the falloff in κ is affected by the temporal pulse shape though κ in the dominant central region depends only on the integrated area of the pulse.

The experimental study of this problem proceeds from the basic system used previously to study dynamical localization in a spatially modulated standing wave [4–6]. The experiments are performed with ultracold sodium atoms trapped and laser cooled in a room temperature, UHV magneto-optic cell trap (MOT) [7]. A magnetic field gradient of 10 G/cm for trapping is provided by a pair of anti-Helmholtz coils. Residual magnetic fields are nulled by three-axis Helmholtz coils which surround the quartz envelope. A stabilized single-mode dye laser ($L1$) at 589 nm, pumped by an argon ion laser, is used for cooling, trapping, and detection of the sodium atoms. The main beam from this laser passes through a resonant $LiTaO_3$ electro-optic phase modulator which is driven at 1.712 GHz. This imposes 15% rf sidebands on the laser, and prevents optical pumping of the sodium atoms into the $F = 1$ ground state during the cooling stage.

 0031-9007/95/75(25)/4598(4)$06.00

The beam then passes through an 80 MHz acousto-optic modulator (AOM1) which is used as a shutter and to stabilize the intensity fluctuations of $L1$ at the trap to approximately 1%. After AOM1 the light is coupled into a single-mode polarization-preserving fiber. This beam is servolocked at a detuning of 20 MHz to the red of the $(3S_{1/2}, F = 2) \longrightarrow (3P_{3/2}, F = 3)$ transition at 589 nm. The output of the fiber is collimated to a diameter of 2 cm and split into three pairs of counterpropagating beams. They are polarized in a standard $\sigma^+ - \sigma^-$ configuration, and are aligned to overlap orthogonally in the center of the magnetic field gradient in order to establish the MOT molasses. Approximately 10^5 atoms are trapped within a Gaussian distribution of position ($\sigma = 0.17$ mm) and momentum ($\sigma = 4.6\hbar k_L$). After trapping and cooling, the trap is turned off. The rf sidebands are turned off 15 μs before the light and magnetic field gradient are shut off, in order to pump the atoms into the $F = 1$ ground state. The interaction potential is provided by a second stabilized single-mode dye laser, $L2$ (pumped by the same argon ion laser). The light from $L2$ passes through a fast 80 MHz acousto-optic modulator that has a 25 ns rise time and controls the pulse sequence. The beam is spatially filtered, aligned with the trapped atoms, and then retroreflected from a mirror outside the vacuum chamber to create a standing wave (beam waist 1.2 mm). The phase stability of this setup was measured in optical homodyne to be better than 125 mrad for an interaction time of 100 μs. A fast photodiode detects the pulse train which is digitized, as shown in Fig. 1, and stored in the computer. Each pulse is typically non-Gaussian and the integrated area is used in the comparison with theory. The pulse period, duration, and number of pulses in a burst are variable parameters in the experiment. The probability of spontaneous scattering is below 1% per pulse for the data presented. The detection of momentum is accomplished by letting the atoms drift in the dark for a controlled duration (typically 2.0 ms), after which the trapping beams are turned on in zero magnetic field, forming an optical molasses [7] which freezes the position of the atoms. The region of laser beam overlap in the vacuum is approximately 8 cm^3, which defines the usable volume for atom detection via this "freezing molasses." The atomic position via fluorescence imaging is then recorded in a short (10 ms) exposure on a thermoelectrically cooled charge-coupled device. The final molasses distribution and the free-drift time enable the determination of the total momentum after the initial MOT spatial distribution is deconvolved. In each measurement sequence we alternate between a measurement of the initial MOT momentum distribution and a measurement of the momentum distribution after exposure to the train of pulses.

We show results for $\Omega_{\text{eff}}/2\pi = 75.6$ MHz and $T = 1.58$ μs. Each pulse has a rise and fall time of 25 ns and a temporal full width at half maximum of 100 ns. The effective impulse corresponds to $\kappa = 11.6$ (with an experimental uncertainty of 10%) and the corresponding classical phase portrait is shown in Fig. 2 with the classical boundary at $p/2\hbar k_L \approx 45$. The scaled Planck's constant $\bar{k}$ equals 2.0. For these experimental parameters, the theoretical estimate of the localization length ξ (the $1/e$ point of the momentum distribution) is 8.3 in units of $2\hbar k_L$. The falloff in κ over the localization length is

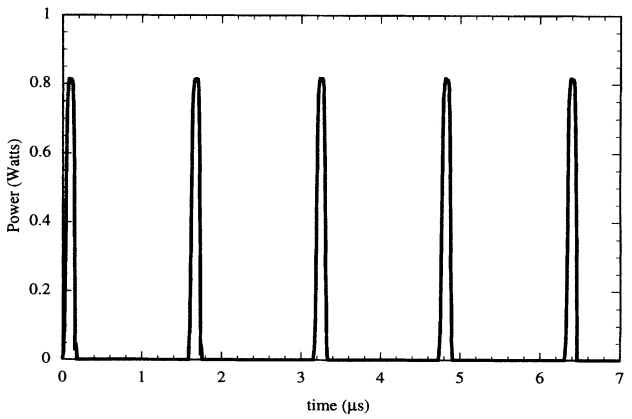

FIG. 1. Digitized temporal profile of the pulse train measured on a fast photodiode. The vertical axis represents the total power in both beams of the standing wave. $f(t)$ and Ω_{eff} are derived from this scan.

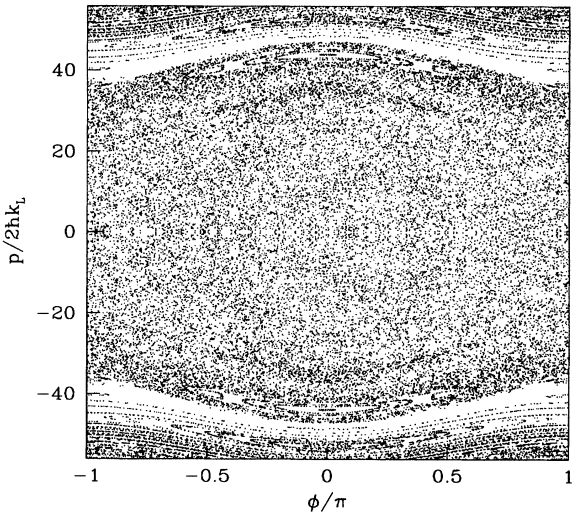

FIG. 2. Classical phase portrait for the pulsed system using a train of Gaussians to represent the experimental sequence. The integrated area under a single pulse is taken to be the same as in the experiment. The standing wave has a spatial rms value of $\Omega_{\text{eff}} = 75.6$ MHz, $T = 1.58$ μs, and $\alpha = 0.027$ leading to $\kappa = 11.6$. Note that a small intensity variation due to spatial overlap of atoms and laser profile results in a somewhat smaller κ than that at peak field.

small, ≈15%. Thus, the experimental conditions are in a regime well described by the QKR.

The momentum distributions were measured for an increasing number of kicks (N), with the pulse height, period, and pulse duration fixed. The line shapes shown in Fig. 3 clearly evolve from an initial Gaussian distribution at $N = 0$ to an exponentially localized distribution after approximately $N = 8$. We have measured distributions out until $N = 50$ and find no further significant change. Since the atoms in the ensemble are independent, these results should represent the single-atom wave function. The growth of $\langle (p/2\hbar k_L)^2 \rangle/2$ as a function of the number of kicks was calculated from the data and is displayed in Fig. 4. It shows diffusive growth initially until *a quantum break time*, after which dynamical localization is observed [2]. Though not shown here, classical and quantum calculations both agree with the data over the diffusive regime. Beyond the quantum break time, the classical energy continues to increase diffusively while the measured line shapes stop growing, in agreement with the quantum prediction. The observed line shape is shown (Fig. 4 inset), and is clearly exponential. These results are the first experimental confirmation of the quantum break time.

Between kicks the atoms undergo free evolution for a fixed duration. The quantum phase accumulated during the free evolution is $e^{-ip^2T/2M\hbar} = e^{-ip^2/2k} = e^{-in^2k/2}$, where n labels the plane-wave basis. A *quantum resonance* occurs when $k/2$ $(= 4\omega_r T)$ is chosen to be a rational multiple of 2π. We have scanned T from 3.3 to 50 μs and find quantum resonances when the quantum phase is an integer multiple of π [8]. For even multiples, the free evolution factor between kicks is unity, and for odd multiples, there is a flipping of sign between each kick. Quantum resonances have been studied theoretically, and it was shown that instead of localization, one expects energy to grow quadratically with time [9]. This picture, however, is only true for an initial plane wave. A general analysis of the quantum resonances shows that for an initial Gaussian wave packet, or for narrow distributions not centered at $p = 0$, the momentum distribution is actually smaller than the exponentially localized one, and settles in after a few kicks [10]. Our experimental results are shown in Fig. 5. Ten quantum resonances are found for T ranging between 5 μs (corresponding to a phase shift of π) and 50 μs (10π) in steps of 5 μs. The saturated momentum line shapes as a function of T are shown in Fig. 5(a). The narrower, nonexponential profiles are the resonances between which the exponentially localized profiles are recovered. The time evolution of the line shape at a particular resonance is shown in Fig. 5(b) from which it is clear that the distribution saturates after very few kicks. We also observe the difference in early time evolution (2 − 3 kicks) when $k/2$ equals odd multiples of π, arising from the alternating sign between kicks.

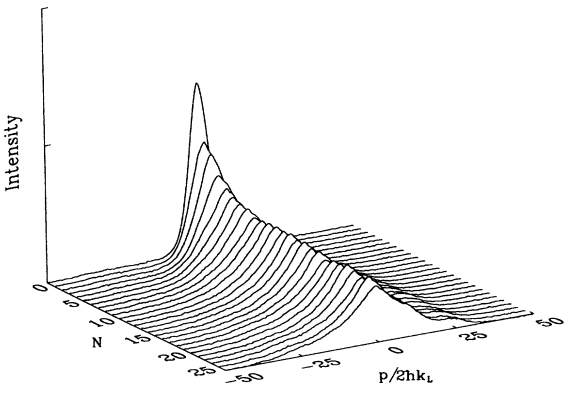

FIG. 3. Experimental time evolution of the line shape from the initial Gaussian until the exponentially localized line shape. The parameters are the same as Fig. 2 with $k = 2.0$. The break time is approximately 8 kicks. Fringes in the freezing molasses lead to small asymmetries in some of the measured momentum line shapes as seen here and in the inset of Fig. 4. The vertical scale is measured in arbitrary units and is linear.

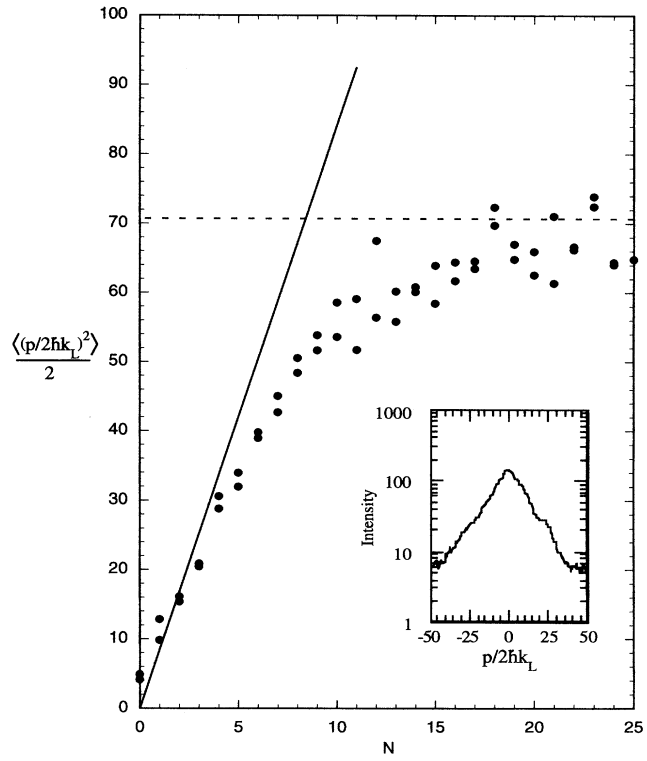

FIG. 4. Energy $\langle (p/2\hbar k_L)^2 \rangle/2$ as a function of time. The solid dots are the experimental results. The solid line shows the calculated linear growth proportional to the classical diffusion constant $\kappa^2/2$. The dashed line is the saturation value computed from the theoretical localization length ξ. The inset shows an experimentally measured exponential line shape on a logarithmic scale which is consistent with the prediction $\xi = \kappa^2/4k^2 \approx 8.3$.

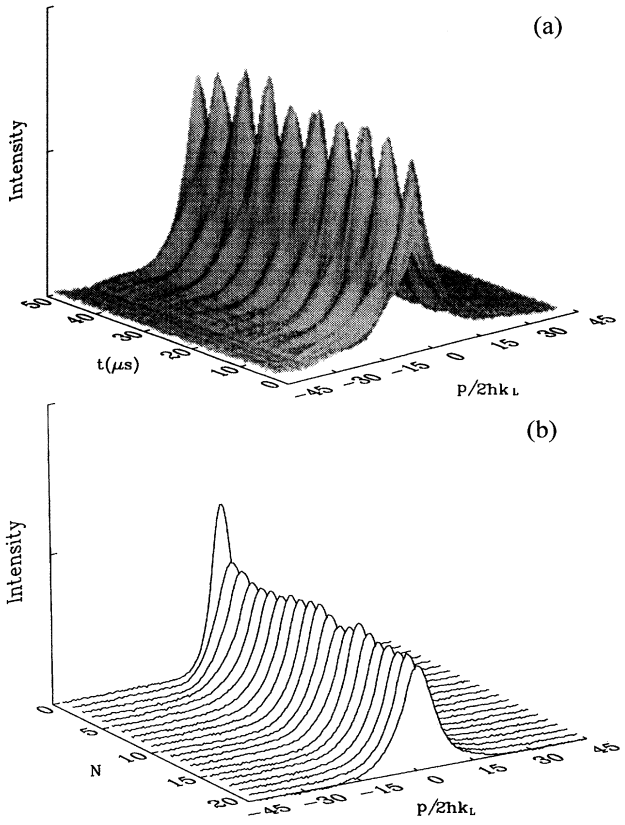

FIG. 5. Experimental observation of quantum resonances: (a) Occurrence as a function of the periodicity of the pulses. The surface plot is constructed from 150 line shapes measured, for each T, after 25 kicks. This value of N ensures that the line shapes are saturated for the entire range of T shown. At resonance, the profiles are nonexponential and narrower than the localized shapes which appear off resonance. Note that the vertical scale is linear. (b) Time evolution of a particular resonance ($T = 10$ μs corresponding to $\hbar = 4\pi$). The parameters α and $\Omega_{\text{eff}}/2\pi$ are the same as in the other figures.

In our system the canonical variables are position and momentum, as opposed to angle and angular momentum for the quantized rotor. The observed effects reported here are identical for both systems. However, by adding noise terms that break the spatial periodicity, the quantum dynamics can be substantially different than for a kicked rotor [11,12]. This can be achieved experimentally by adding a standing wave that has a different, incommensurate periodicity. We will study the effects of "symmetry breaking" potentials in the context of noise induced delocalization, and localization in two and three dimensions.

We thank Dr. Steven Wilkinson for a careful reading of the manuscript. We also thank Professor Dima Shepelyansky and Professor Shmuel Fishman for helpful discussions. The work of M. G. R. was supported by ONR, the Robert A. Welch Foundation, and the NSF. The work of B. S. was supported by the NSF.

*Present address: NOAA/CMDL, Nitrous Oxide and Halocompounds Division, Mail Stop R/E/CG1, Boulder, Colorado 80303.

[1] A. L. Lichtenberg and M. A. Lieberman, *Regular and Chaotic Dynamics* (Springer-Verlag, Berlin, 1991).
[2] L. E. Reichl, *The Transition to Chaos in Conservative Classical Systems: Quantum Manifestations* (Springer-Verlag, Berlin, 1992), and references therein.
[3] R. Blümel, S. Fishman, and U. Smilansky, J. Chem. Phys. **84**, 2604 (1986).
[4] R. Graham, M. Schlautmann, and P. Zoller, Phys. Rev. A **45**, R19 (1992).
[5] F. L. Moore, J. C. Robinson, C. Bharucha, P. E. Williams, and M. G. Raizen, Phys. Rev. Lett. **73**, 2974 (1994); J. C. Robinson, C. Bharucha, F. L. Moore, R. Jahnke, G. A. Georgakis, Q. Niu, M. G. Raizen, and Bala Sundaram, Phys. Rev. Lett. **74**, 3963 (1995); this work was reviewed in Phys. Today **48**, No. 6, 18 (1995).
[6] P. J. Bardroff, I. Bialynicki-Birula, D. S. Krähmer, G. Kurizki, E. Mayr, P. Stifter, and W. P. Schleich, Phys. Rev. Lett. **74**, 3959 (1995).
[7] Laser cooling and trapping is reviewed by Steven Chu in Science **253**, 861 (1991).
[8] Other resonances should occur for $\hbar = 2\pi r/s$ but these are not resolved experimentally.
[9] F. M. Izrailev and D. L. Shepelyansky, Sov. Phys. Dokl. **24**, 996 (1979); Theor. Math. Phys. **43**, 553 (1980).
[10] Q. Niu and Bala Sundaram (to be published).
[11] S. Fishman and D. L. Shepelyansky, Europhys. Lett. **16**, 643 (1991).
[12] D. Cohen, Phys. Rev. A **44**, 2292 (1991).

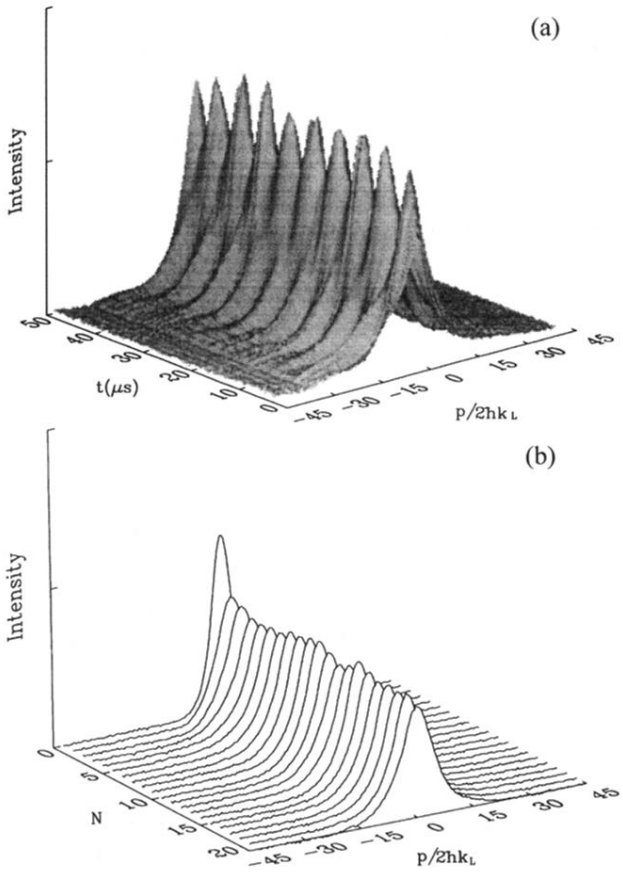

FIG. 5. Experimental observation of quantum resonances: (a) Occurrence as a function of the periodicity of the pulses. The surface plot is constructed from 150 line shapes measured, for each T, after 25 kicks. This value of N ensures that the line shapes are saturated for the entire range of T shown. At resonance, the profiles are nonexponential and narrower than the localized shapes which appear off resonance. Note that the vertical scale is linear. (b) Time evolution of a particular resonance ($T = 10\ \mu$s corresponding to $k = 4\pi$). The parameters α and $\Omega_{\text{eff}}/2\pi$ are the same as in the other figures.